

Full Length Research Paper

Seasonal variability of rainfall and thunderstorm in Guinea over the period 1981 to 2010

**Ibrahima Kalil Kante^{1,2,3*}, Saïdou Moustapha Sall¹, Daouda Badiane¹, Idrissa Diaby² and
Ibrahima Diouf^{1,4}**

¹Laboratoire de Physique de l'Atmosphère et de l'Océan, Université Cheikh Anta Diop, Senegal.

²Laboratoire de l'Enseignement et de Recherche en Energetique Appliquée, Université de Conakry, Guinée.

³Direction Nationale de la Météorologie de Guinée, Face Jardin 2 octobre, Conakry. BP: 566, Guinée.

⁴NOAA Center for Weather and Climate Prediction, 5830 University Research Court, College Park, Maryland 20 740, USA.

Received 26 March, 2019; Accepted 12 July, 2019

Republic of Guinea is one of the West African countries which share form a border with the southern part of the Sahel. It is located in the tropical area where the convective systems activities are intense with strong rainfall. Our results on Standardized Precipitation Index are coherent with the Sahel drought during the 1970s, and a recovery period of rainfall since the last years. The Standardized Thunderstorms Index shows positive anomalies (1981-1997) corresponding to the dry period of rainfall, while a negative anomalies is shown (1998-2010) for the wet period. This study highlights the relationship between thunderstorms and rainfall amounts in Guinea in the context of climate variability. Indeed, by categorizing the rainfall in two groups respectively weak and heavy, we calculated their correlations with thunderstorms. We found significant correlations between weak rainfall and thunderstorms. To appreciate the findings with the standardized anomalies of precipitation and thunderstorms, we also performed Rotations of Empirical Orthogonal Function and Principal Component Analysis to identify the coherent mode of the interannual variability of these parameters. We found that the first mode is the best Empirical Orthogonal Function which is coherent with is the results shown by the Standardized Index of Precipitation and Thunderstorms. To check the significance of each Empirical Orthogonal Function mode, we use the North's rule of thumb for estimating the sampling errors. It was noticed that no modes was concerned by sampling errors. And then, the rainfall seasonal cycle shows a unimodal rainfall regime, while the thunderstorms' one indicates a bimodal cycle. Our study could improve knowledge about rainfall amounts and thunderstorms variability, especially in climatic variability context.

Key words: Rainfall, thunderstorm, spatio-temporal variability, correlation.

INTRODUCTION

Republic of Guinea is one of the wettest countries in West Africa. The average of its rainfall amount can exceed 3000 mm per year. During the twentieth century, there was a decrease of rainfall amounts in most of the

West African countries (Zhou et al., 2008). Indeed, the Figure 1 shows that despite heavy rainfall observed in Guinea, but the latter experienced a very marked rainfall decrease during the first decade of our study period

(1981-1991). This rainfall decrease is due to an overall reduction of rainfall in West African area. The marked rainfall decrease during the first over our area of study is consistent with findings from the Fifth Assessment Report (AR5) of the Intergovernmental Panel on Climate Change (Smith et al., 2014), which highlighted that the West Africa region suffered changes due to natural and anthropogenic forcing. Nevertheless, there is still a large debate about the impact of anthropogenic climate change on decadal to multi-decadal rainfall variability over the West Africa (Nicholson et al., 2000; Giannini et al., 2003; Mohino et al., 2010). These changes have altered the rainfall distribution that presents large decadal and interannual variability. The decadal signal is modulated by anthropogenic factors, but also by large modes of natural variability, such as the Atlantic Multidecadal Oscillation. The interannual signal is mainly affected by the El Niño Southern Oscillation, the Tropical Atlantic basin, and internal atmospheric variability over the region. This is coherent with several works done on the Sahel rainfall where the 1970s correspond with a drought from 1970 to 1992, like (Solomon et al., 2007; Grist and Nicholson 2001; Nicholson et al., 2013; Hulme, 1992; Lamb and Peppler, 1992; Janicot and Fontaine, 1993; Le Barbe et al., 2002). Since the beginning of the 2000s, there is an improved rainfall trend in the central region of the Sahel (Ali et al., 2000; Nicholson et al., 2005), with a very wet year 1994. Guinea experienced this return to normal rainfall in the year 1994 significantly wet also (Figure 1).

In Guinea, rainfall is very important for the population's activities and ecosystems. Therefore, it defines different geophysical regions (Loua et al., 2017). Rainfall events are usually associated with meso-scale convective systems (MCS); especially that are the most frequently observed rainfall systems in the Sudano-Sahelian belt (Laurent et al., 1998; Laing et al., 1999). These rainfall events over tropical Africa and the Atlantic during the West African Monsoon period (WAM) are accompanied by thunderstorms. Many interesting results have been obtained from correlations between lightning activities and radar reflectivity, and between lightning and precipitation activities (Sheridan et al., 1997; Petersen and Rutledge, 1998; Soula et al., 1998; Zhou et al., 2002). These results exhibit a strong relationship between the raining convective system, lightning frequency and the intensity of precipitation (Béavogui et al., 2011). However, the relationship between thunderstorms and rainfall amounts is less documented in our area of study (Guinea). It is in this perspective, that we performed a climatological approach by studying this phenomenon in Guinea by considering 4 synoptic stations including one from each geophysical region. As

part of this work, we consider the 12 synoptic stations of Guinea from four geophysical regions, having in each of them three stations. The main objective is to better understand the rainfall variability of Guinea in relation with the thunderstorms and to analyze the Empirical Orthogonal Function (EOF)/Principal Component (PC) to identify the coherent mode of interannual variability of them.

MATERIALS

Area of study

The area of study is as shown in Figure 2, located between the latitudes 7°N and 13°N, and the longitudes 15°W and 7°W. The Republic of Guinea is a West African country, with an estimated area of 245,857 km². It is subdivided into four geophysical regions: Lower-Guinea (LG, hereafter), Middle Guinea (MG, hereafter), Upper-Guinea Guinea (UG, hereafter) and Forest-Guinea (FG, hereafter). Each geophysical region has three synoptic weather stations.

The naming of the geophysical regions LG, MG, UG and FG is in accordance with their climate and topography.

The LG includes the synoptic weather stations of Boké, Conakry and Kindia; also called Maritime-Guinea because of its coastal position (near the sea). It is the coastal strip between Guinea - Bissau in the north and Sierra Leone in the south (around 300 km), about 100 to 150 km wide. It covers 15% of the country's total area. The marine marshes occupy around 360 000 ha area, including 260 000 ha of mangroves, the largest in West Africa (Frenken, 2005). It has a wet tropical climate, with rainfall reaching its maximum in August and can exceed 4,000 mm/year in Conakry.

The MG region includes the synoptic stations of Koundara, Labé and Mamou. It covers 26% of the country's total area. Fouta-Djalou massif occupy around 80 000 km² around and its highest point is Mount Loura (1 532 m), including the most mountainous region of Guinea. Its soil consists mainly of stepped plateaus often over 1000 m notched by valleys, dominating plains and depressions with an altitude exceeding 750 m and can exceed 1200 m in some places (Frenken, 2005). It is in this region where many rivers and streams of West Africa take their sources: Senegal and Gambia Rivers in the north, Koliba, Rio Grande, Fatale and Konkouré Rivers in the west, the Kaba Rivers, Kolente to the south, and Niger to the east. Its climate is marked by a relatively high day time thermal amplitude of up to 19°C at Labé.

The rainy season can range from five to eight months between Koundara and Mamou with an amount rainfall less than 1,300 mm to the north.

The UG region includes the synoptic stations of Faranah, Kankan and Siguiri covers 39% of country's total area. It is located between Guinea-Forest and Fouta-Djalou on the western edge of the Niger's vast basin. This region, with an average altitude of 500 m, has a slight relief which explains the rivers spreading. Its climate is Sudanian with an annual rainfall between 1600 mm in the south and 1200 mm in the north. It represents the arid or Sahelian area of Guinea because of the similarity of its climate with Sahel. Featuring a grassy savanna with plateaus and river plains (River Milo) that is rich in agriculture. While, seasonal thermal amplitude is

*Corresponding author. E-mail: ibrahima.kante@ucad.edu.sn. Tel: +221-77-305-94-03.

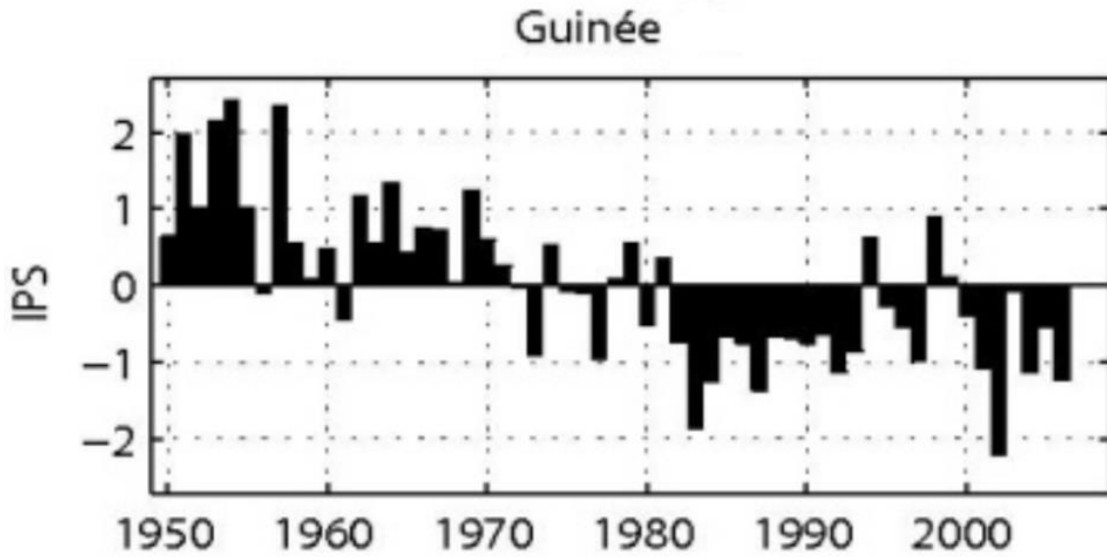


Figure 1. Standardized Precipitation Index (SPI) in Republic of Guinea from 1951 to 2010 (Louvet et al., 2011). The X and Y axis are years and anomalies respectively.

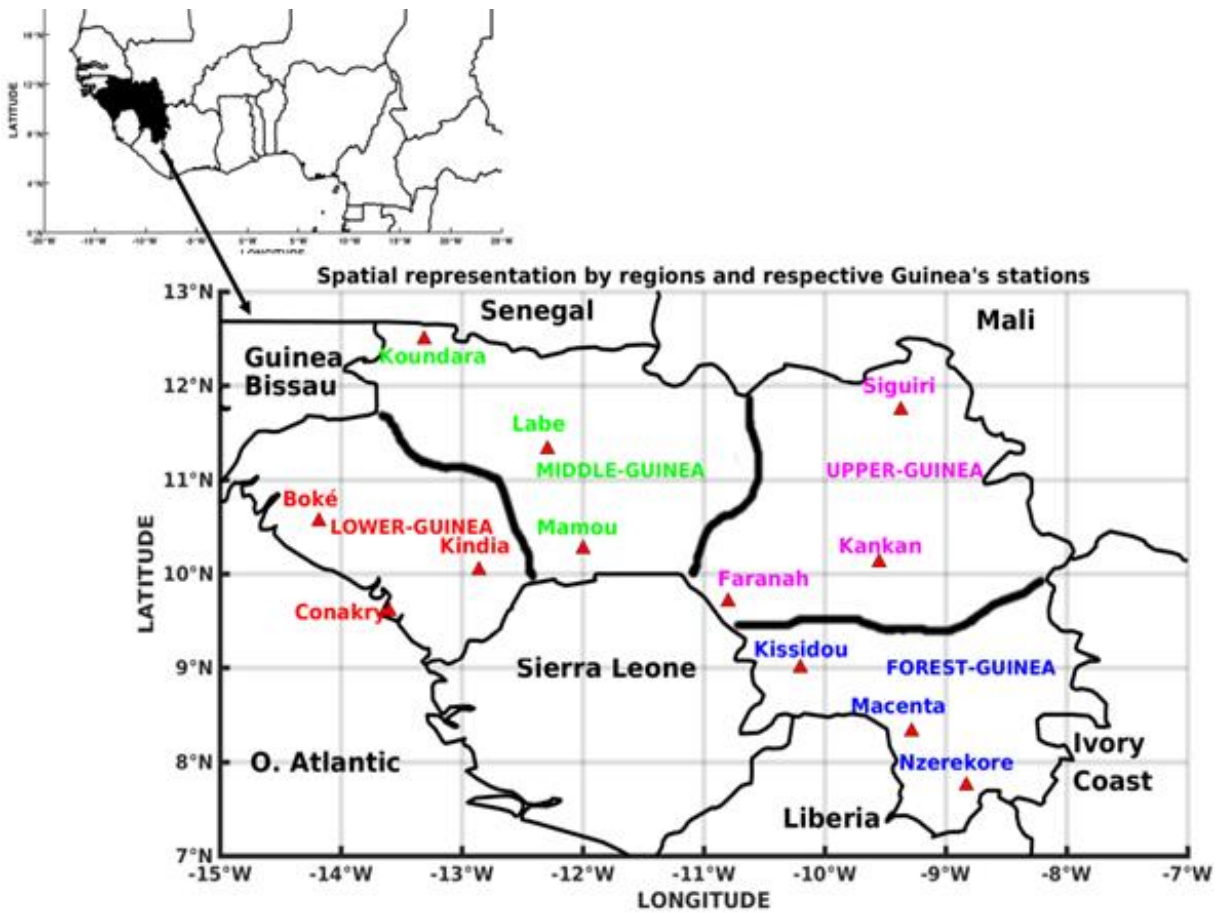


Figure 2. Meteorological observation stations. The map shows the meteorological stations locations used for the four (4) geophysical regions of Guinea: Low-Guinea (Boke, Conakry, Kindia), Middle-Guinea (Koundara, Mamou, Labe), Upper-Guinea (Faranah, Kankan, Siguiri) and Forest-Guinea (Kissidou, Nzerekore, Macenta).

Table 1. Situation of the available datasets by station, timescale and time period.

Station		Latitudes	Longitude	Altitude (m)	Parameters (monthly)	Time period
Low Guinea	Boke	10°56'	-14°18'	69	Rainfall - Thunderstorm	1981-2010
	Conakry	09°64'	-13°58'	46	Rainfall - Thunderstorm	1981-2010
	Kindia	10°04'	-12°86'	458	Rainfall - Thunderstorm	1981-2010
Middle Guinea	Koundara	12°34'	-13°31'	90	Rainfall - Thunderstorm	1981-2010
	Labe	11°19'	-12°29'	1050	Rainfall - Thunderstorm	1981-2010
	Mamou	10°38'	-10°08'	782	Rainfall - Thunderstorm	1981-2010
Upper Guinea	Faranah	10°26'	-10°80'	358	Rainfall - Thunderstorm	1981-2010
	Kankan	10°12'	-9°55'	376	Rainfall - Thunderstorm	1981-2010
	Siguiri	11°74'	-9°37'	361	Rainfall - Thunderstorm	1981-2010
Forest Guinea	Kissidou	09°19'	-10°11'	524	Rainfall - Thunderstorm	1981-2010
	Macenta	08°32'	-9°28'	542	Rainfall - Thunderstorm	1981-2010
	Nzérékoré	07°75'	-8°83'	467	Rainfall - Thunderstorm	1981-2010

important, extreme temperatures can vary from 14°C in the rainy season to 37°C in the dry season.

The FG region includes the synoptic weather stations of Kissidou, Macenta and Nzérékoré. This region corresponds to the southern part of Guinea and covers 20% of the area total of country. Its relief presence two mountains namely Mount Simandou and Mount Nimba, the latter is the highest in the country with 1,752 m altitude. The Mont Nimba Strict Nature Reserve is a UNESCO World Heritage Site and covers most of the ecotope, which is home to more than 200 endemic species: duikers, big cats (lions and leopards), civets, and two species of viviparous amphibians (Frenken, 2005). This region also enjoys a climate characterized by an unusually long rainy season (between seven and nine months) than LG, MG and UG. The Ziama Massif Biosphere Reserve is home to more than 1,300 plants species and more than 500 animal species.

Data

Observation data provided by the Guinea National Meteorology Service (GNMS) are used. Guinea's meteorological observation network has a very low density due to obsolete meteorological tools equipments and lack of performing weather observers. Many of these stations have several data gaps, which sometimes complicate the use of these data. For this purpose, twelve (12) synoptic stations (Figure 2) are selected for this study in which observation network is regular, and its data are trustworthy. These are monthly rainfall and thunderstorm data for 1981-2010 period (Table 1).

For thunderstorm data during 24 h of observations, at least one thunderstorm occurs that day is considered as a stormy day. Sometimes, thunderstorms can be observed without having rainfall at a given station. But there may be rains far from station, and this rainfall is not observed at station. However, to evaluate these thunderstorm data we compared to the ones estimated by Tropical Rainfall Measuring Mission (TRMM) which have resolution of 0.1 × 0.1 covering 1998-2013 period (Figure 3). They are called Lightning Imaging Sensor (LIS, hereafter) data. LIS is a scientific instrument integrated into the TRMM satellite, its data is used to detect deep convection without earth-ocean bias, to estimate the rainfall mass in the region and to multi-phase thunderstorm clouds with a weak vertical movement (Christian et al., 1999). The LIS 0.1

Degree Very High-Resolution Gridded Lightning Monthly Climatology (VHRMC) dataset consists of gridded monthly total lightning flash rates seen by LIS (NASA). This information can be used for severe thunderstorm detection and analysis, and also for lightning-atmosphere interaction studies (Rakov and Uman, 2003). We noticed in the four regions that, LIS data reproduce quite well the observations. Otherwise, the TRMM underestimated observations, but the peaks at the beginning of season (May or June) and its end of season (October) are coherent. We noticed likewise with minima which are observed in July or August.

In this purpose, we have considered 30-year climatological series recommended by World Meteorology Organization (WMO), which are the monthly cumulative data. These are the monthly cumulative of these data that we use in this work over the period 1981-2010. They are used to calculate the standardized index, seasonal cycle and interannual variability to investigate the spatio-temporal variability. And then, EOF and PC variables, correlation coefficients and a significance statistical test are used to better understand the relationship between rainfall and thunderstorms.

METHODS

The first part refers to the calculation of the Standardized Precipitation Index (SPI, hereafter), and Standardized Thunderstorms Index (STI, hereafter). The SPI is an index calculation method created by McKee et al. (1993) (Equation 1). This statistical method allows to characterize the wet and dry period in a given rainfall data series, with respect to climatology (Ali et al., 2009). The usual manner of calculating the SPI is to average the standardized rainfall at each rainfall station for a given year. It quantifies also observed precipitation as a standardized departure from a selected probability distribution function that model the raw precipitation data (Keyantash and Dracup 2002). The SPI values can be interpreted as the number of standard deviations by which the observed anomaly deviates from the long-term mean (Ali et al., 2008). This index is often used in a very simple way by evaluating the rainy season (Keyantash and Dracup 2002). The rainfall series is wet if the SPI is greater than 0, and dry if the SPI is less than 0.

We applied the same thing on thunderstorms data for obtaining the STI. It also reports on the downward multi-year variability of thunderstorms and the return to normal values in Guinea.

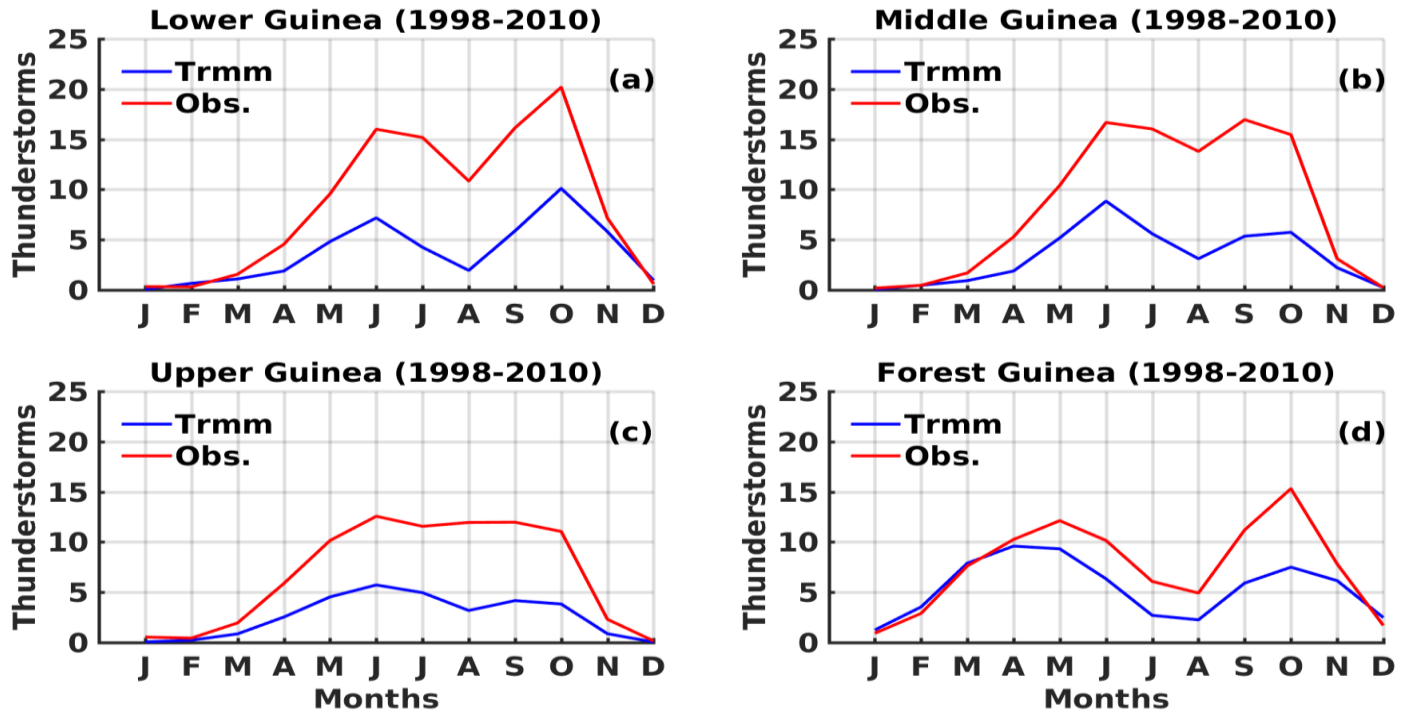


Figure 3. Comparison of seasonal cycles of thunderstorms (observation, red curve) and Lightnings (satellite, blue curve) in Guinea over 1998-2010 period. The X and Y axis are months and thunderstorms respectively.

$$I_i = \frac{X_i - \bar{X}}{\sigma} \tag{1}$$

where I_i : the calculated standardize index of the considered variable for a given year i ; X_i : the annual value of the considered variable X for a given year i . \bar{x} : the calculated mean of all values of data set X of the considered variable. X_i . σ : Standard deviation calculated from the considered variable X .

The second part of the method focuses on the seasonal cycle of rainfall and thunderstorms in Guinea. It concerns rainfall amount and thunderstorms variabilities during the period 1981-2010. We evaluate the temporal evolution over the studied period of the rainfall and thunderstorms means in geophysical regions of Guinea using the spatial means of the 3 stations located in these regions. This allow us to determine the beginning and end of rainfall and thunderstorm seasons in Guinea.

The third part presents EOFs and PCs for our rainfall and thunderstorm series in Guinea. To realize this, the variables considered are the rainfall amount and thunderstorm occurrences at the twelve (12) stations. But before our analysis, we removed the trends in respectively rainfall and thunderstorm data. The decomposition of a set of complex data varying in time and space into a set of EOFs and time series of associated principal components provides a better understanding of the main modes of spatial variability (Deser and Blackmon 1995). This linear method is widely used in climatology for the processing of heterogeneous data (Richman, 1981). A basic method of data analysis was considered by Bourcoche and Saporta, (1987) and Dawson (2016). The EOFs and PCs of a dataset describe a new base where, instead of a series of time-varying spatial observations, the dataset is represented as a set of fixed spatial patterns or modes, which represent a given amount of total variance. It allows extracting the

maximum information, in simple form, from a very important dataset; it will highlight the inter-relationships between the variables and similarities or oppositions between observations (Poccard-Leclercq 2000). All of this data and a set of time series describe how each pattern changed over time. The method of this analysis is purely mathematical and does not depend on any physical property of the analyzed quantity (Abdi and Williams, 2010) applications, the first EOFs accounts for a large part of the total variance, allowing the study of one or two modes to provide insight into the variability embedded in the dataset (Deser and Blackmon 1995). The first mode EOF1 is the time series index that produces regression/correlation maps with the overall strongest amplitudes of data. The second one EOF2 is the time series index that produces regression/correlation maps with the overall strongest amplitudes after the variability associated with EOF1 is subtracted out of the data. And so on and so forth for modes EOFs 3 and 4. In short terms, the PCs are the main components, EOFs are the eigenvectors and the percentages obtained by modes are the eigenvalues (variance). Each empirical mode is formed by a space pattern and a time series which are derived from the eigenvalues and eigenvectors of the covariance (or correlation) matrix (Cattell, 1966). In recent years, the EOFs technique has been largely used to identify potential physical modes (Mestas-Nunez 2000). The problems that may arise by using EOFs or rotated EOFs is discussed by several authors. In Dommenget and Latif (2002) and North et al. (1982) main statistical uncertainty in the estimation of the EOFs is discussed. In the standard EOF analysis, it is assumed that the modes are orthogonal in space and time, and that the first mode is the one that maximizes the explained variance over the total dataset (Mestas-Nunez 2000). An overview of the different ways in rotating EOFs or defining the varimax rotation can be found in Richman (1986), North et al. (1982) and Kaiser et al. (1958). In our study, it is the varimax method that we use to get rotations of EOFs (REOFs) and PCs (RPCs) before plotting them.

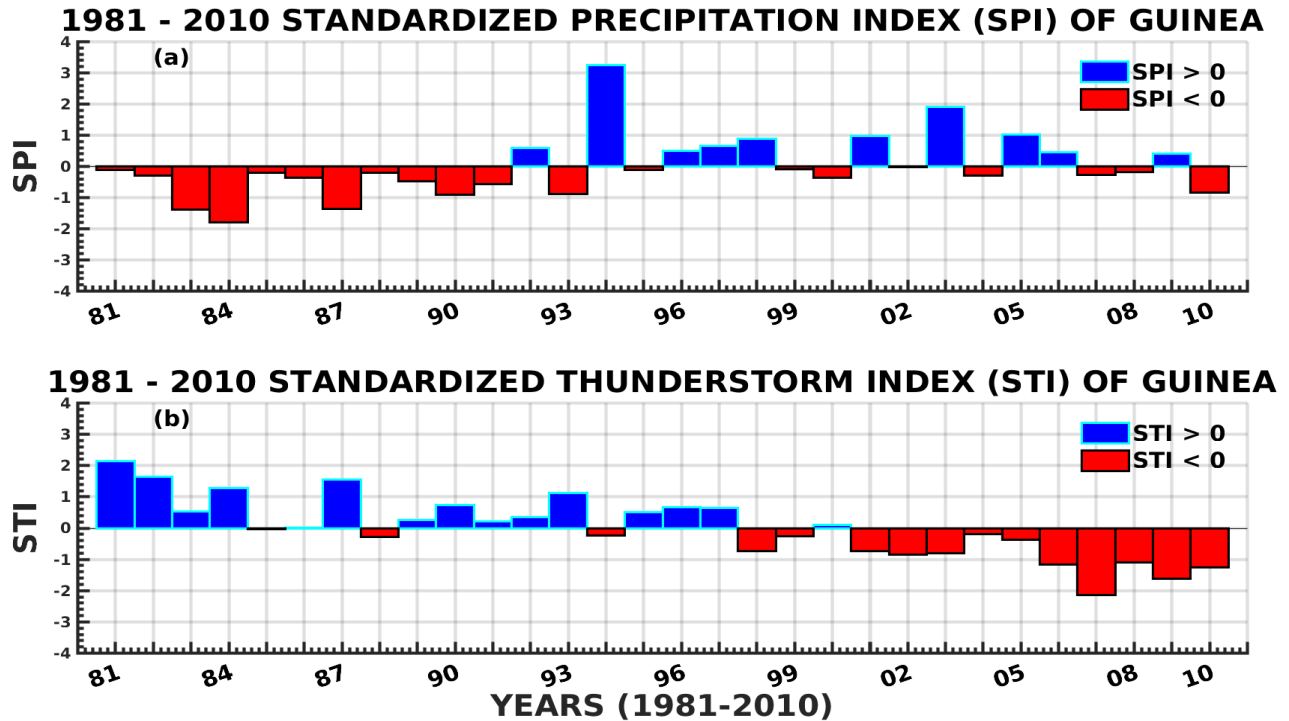


Figure 4. Standardized Precipitation Index (mm) and Standardized Thunderstorms Index (occurrence number). The X and Y axes are years and anomalies respectively. (a) Standardized Precipitation Index (SPI), and (b) Standardized Thunderstorms Index (STI) in Guinea, for the period 1981-2010.

The statistical significance thresholds used to capture the number principal components are given by the scree test (Mestas-Nunez 2000) and the North test (Dommenget and Latif 2002). We use North's rule of thumb for estimating the sampling errors (Equation 2) to test the significance of each EOF mode. The rule is simply that if the sampling errors of a particular eigenvalue $\Delta\lambda$ are comparable to or larger than the spacing between λ and a neighboring eigenvalue, then the sampling errors for the EOF associated with λ will be comparable to the size of the neighboring EOF (Dommenget and Latif 2002). $\Delta\lambda$, allows also to determine the 95% significance errors in the estimation of the eigenvalues. The analysis of these results makes it possible to choose among the four modes of analysis considered which better interpret the rainfall and thunderstorm variability in Guinea. Here we would like to focus on problems of the EOF technique that are not due to statistical uncertainties and more inherent to the method itself (Dommenget and Latif 2002).

$$\Delta\lambda = \lambda\sqrt{2/N} \quad (2)$$

where λ : Eigenvalues of variances (%). $\Delta\lambda$: Samples errors of eigenvalues (%). N: Corresponding to number of modes.

Finally, the fourth method shows the link that could exist between rainfall amounts and thunderstorms. We first considered the rainfall and thunderstorms variables in two classes as in weak rainfall-thunderstorm (0-300 mm) and heavy rainfall-thunderstorm (300-600 mm). In Guinea, the weak daily rainfall amount is around 10 mm/day on average. Multiplying 10 mm by 30 days, we get 300 mm/month, that is, why we considered here 0-300 mm like weak rainfall and 300-600 mm likewise heavy rainfall. We also correlated large rainfall between 600 and 1200 mm, which is not presented in

this document. The correlation coefficients allow us to determine the links between rainfall-thunderstorms and associated levels of significance. In the statistical data analysis, the following formula is used to find respectively the correlation (Equation 3) between the data sets and student test.

$$r = \frac{1}{N} \sum_{i=1}^N \frac{(x_i - \bar{x})}{\sigma_x} \frac{(y_i - \bar{y})}{\sigma_y} \quad (3)$$

where x_i : cumulative of the whole series of the first variable; y_i : cumulative of the whole series of the second variable; \bar{x} : Calculated mean of all values of the data set x_i for the first variable; \bar{y} : Calculated mean of all values of the data set y_i for the second variable; σ_x : Sample standard deviation of all of the first variable x ; σ_y : Sample standard deviation of all of the second variable y ; r : Correlation coefficient, $-1 < r < 1$; N: the total number of values in the set of paired x and y data.

RESULTS AND DISCUSSION

The SPI (Figure 4a) of Guinea over the period 1981-2010 shows a rainfall deficit for the decade (1981-1990) corresponding to a drought period. These observed negative anomalies are coherent with the severe drought in the Sahel in the 1970's to 1991 but that was delayed for a decade (Nicholson et al., 2005). After about the 25

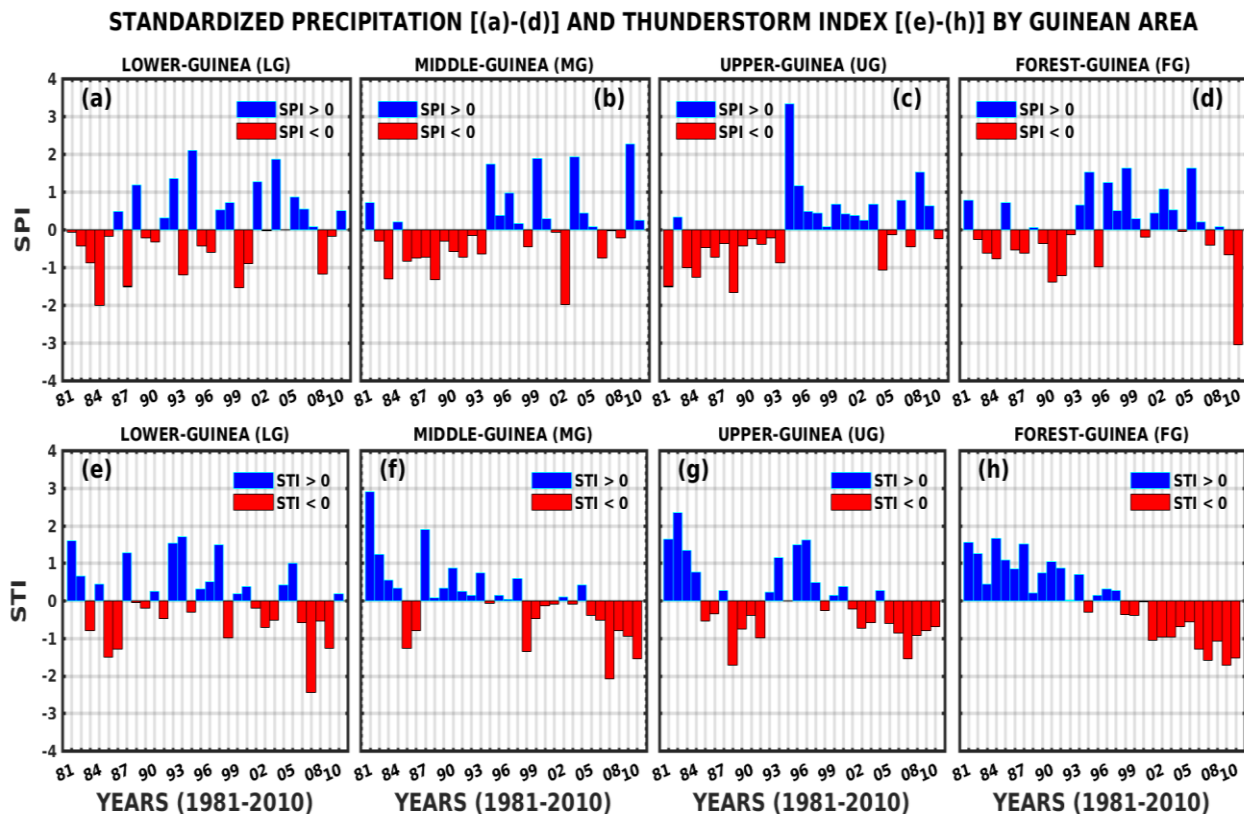


Figure 5. Standardized Precipitation Index (SPI) and Standardized Thunderstorms Index (STI). The X and Y axis are years and anomalies respectively. Standardized Precipitation Index [(a)-(d)] and Standardized Thunderstorms Index [(e)-(h)] by geophysical region of Guinea: Lower Guinea (LG), Middle Guinea (MG), Upper Guinea (UG), and Forest Guinea (FG).

dry years (1965-1990) in the Sahel, the wet years are mainly observed from 1994 (Ali et al., 2009). For the Guinea, the wet period is observed from 1992 up to 2010, with year 1994 showing an important positive peak. This finding over the Sahel is confirmed by other studies like in Ali et al. (2009) and Nicholson et al. (2005), but for Guinea area also, located next to Sahel, our study is among the first revealing this rainfall variability.

Nevertheless, the STI (Figure 4b) for Guinea, shows that the period 1981-1997 was regularly marked by positive thunderstorms anomalies corresponding to the dry period in term of rainfall. This could be caused by the frequency of dry thunderstorms which are not accompanied with rainfall. The overall STI variability indicates also negative anomalies during the period 1998-2010 corresponding to the wet period (Figure 3a).

To refine these results, we have categorized rainfall data in two groups: respectively weak (0-300 mm) and heavy (300-600 mm). Then we correlated these two rainfall categories with the corresponding thunderstorms to understand which is well correlated with thunderstorms (Relationship between rainfall and thunderstorms in Guinea, Sections). The years 1981, 1982, 1984 and 1987 are particularly very wet. Similarly, the years 2006,

2007, 2009 and 2010 reveal negative rainfall anomalies. This situation shows a downward trend in the thunderstorm's regime in Guinea during the period considered for this study.

Standardized index of rainfall and thunderstorms of Guinean regions

In the following, we indicate rainfall and thunderstorms variability in the four natural Guinean regions.

Standardized Precipitation Index (SPI) of Guinean regions

The results show dry and wet periods of rainfall observed in Guinea in each region during 1981-2010. In MG region (Figure 5b) located near the Fouta Djallon Mountains, we have a rainfall deficit during the decade 1981-1992. The UG region (Figure 5c) shows a rainfall deficit also for decade 1981-1993. The UG region is considered as the Guinea region with rainfall characteristic similar to Sahelian one. We noted that 1994, 1999, 2003 and 2009

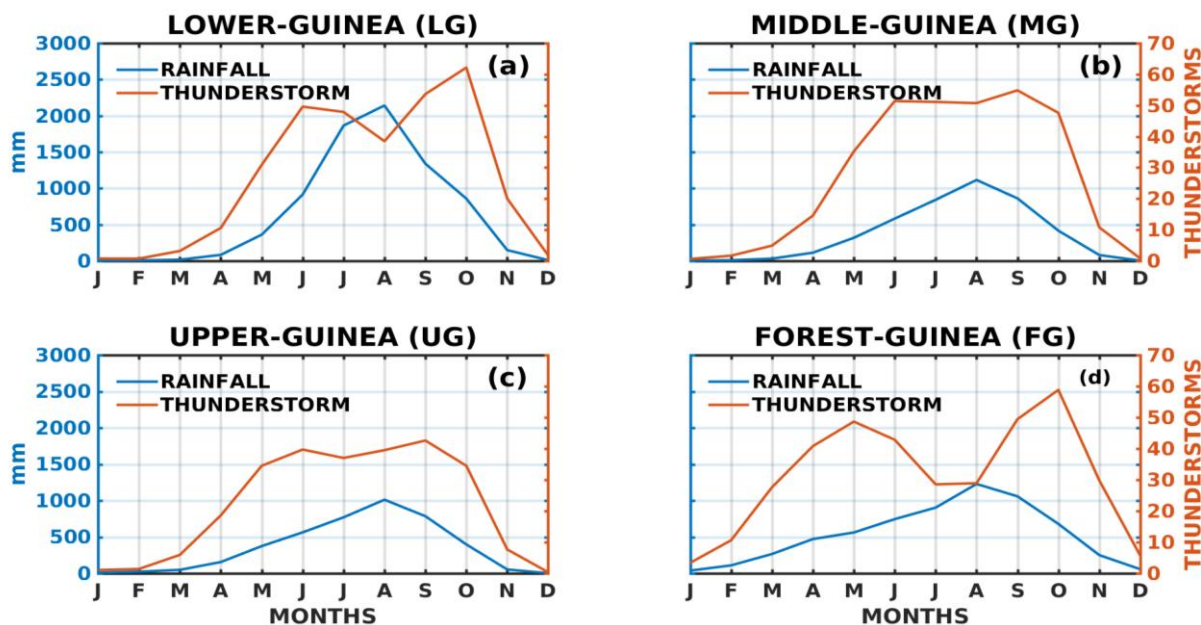


Figure 6. Seasonal cycles of rainfall (blue curve) and thunderstorms (red curve) in the different Guinean regions: (a) Low-Guinea, (b) Middle-Guinea, (c) Upper-Guinea, (d) Forest-Guinea. The X-axis in red and blue are respectively rainfall and thunderstorms. The Y axes are the years.

were particularly wet in MG region. And then, some wet years like 1994, 1995, 2008 and 2009 where 1994 were very wet in the UG region. This confirms that these two regions have shown the same rainfall variability that Guinea has underwent.

LG region (Figure 5a) and FG region (Figure 5d) have shown also this rainfall variability but not like MG and UG. While in FG region (Figure 5d), it is in the decade 1982-1992 that we note important negative rainfall anomalies and 2010 was particularly very dry. Over the LG region, 1984, 1987, 1993, 1999 and 2008 were particularly very dry during the observed drought in Guinea. This would mean that these regions have also suffered the same rainfall deficits and the return to normal rainfall as in Guinea.

Standardized Thunderstorms Index (STI) of Guinean regions

We have a remarkable decreasing thunderstorm activity observed in each region during 1981-2010. Figure 5e to 5h represents STI evolution for the four geophysical regions of Guinea, respectively. In the LG region (Figure 5e), we observed thunderstorms deficits during the years 1981, 1987, 1992, 1993 and 1997 for this coastal area of Guinea, while thunderstorm surplus is found during the years 1985, 1986, 2007 and 2009. The situation of this region shows us that it is not concerned by this thunderstorm rate decreasing.

The STI in the MG region (Figure 5f), UG region

(Figure 5g) and FG region (Figure 5h) region reveal deficits of thunderstorms during last decade (2000-2010). This confirms that these three regions have undergone this thunderstorm variability that Guinea has experienced. These regions have also experienced important negative thunderstorm anomalies namely during 1985, 1998, 2007 and 2010. For this purpose, we note in the Fouta Djallon region (MG), large thunderstorms surpluses recorded in 1981 and 1987. In the UG region (Figure 5g), surpluses and deficits (1988-1992) thunderstorm are alternatively shown, respectively in 1981-1985, 1993-1996 and 1988-1992. Whereas the STI in FG region (Figure 5h) indicates that the forest region is the only one with consecutive years with annual thunderstorms above average from 1981 up to 1991. The situation of this region shows that it is not concerned by the thunderstorms decreasing.

In summary, a multi-year of thunderstorms decreasing is observed in these three regions (MG, UG, FG), this is consistent with what has been observed in a general way about Guinea (Figure 5).

Seasonal mean cycles of rainfall and thunderstorms in Guinea

Considering each natural Guinean region, we show the seasonality of rainfall and thunderstorms. The Figure 6 indicates that Guinea rainfall (blue curve) and thunderstorms (red curve) have respectively unimodal and bimodal variabilities.

Figure 6a and b, respectively for the LG and MG regions, represent the seasonal mean cycles of rainfall

and thunderstorms. The seasonal mean cycle of rainfall is illustrated with a peak in August ranging up to 2200 and 1100 mm, respectively for LG and MG. Moreover, in LG, even if the largest of rainfall amount is found in August, month of July is also wet with a monthly amount close to the August peak. We noticed that July's rainfall of this region amount is larger than the peak of the other regions. The rainy season starts at the coast (LG), at Fouta Djallon (MG) and ends at the same moment, respectively in April and November. Otherwise, regarding the thunderstorms, these LG and MG regions present two peaks, respectively at the beginning and end of the season. They (LG, MG) both have a first peak in June (beginning of season) and a second peak (end of season), respectively in October and September. The months of March and November are respectively the start and the end of thunderstorms events in these two regions.

Figure 6c and 6d, respectively for the UG and FG regions, indicates the seasonal mean cycle for rainfall and thunderstorms. The seasonal mean cycle of rainfall is highlighted with a peak in August ranging up to 1000 and 1200 mm, respectively for UG and FG regions. In the UG region, the rainy season starts in April and ends in October, while in the FG, February and November are, respectively the starting and ending of the rainy season. In FG region, the rainfall can be extended up to ten months e.g. from February to November. Regarding the thunderstorms, seasonal mean cycle presents two peaks the first one at the beginning and the second one at end of season. In UG region, the thunderstorms peaks are observed in June (beginning season) and in September (ending season), while in FG, they are recorded in the earlier in May (beginning season) and end in October (ending season).

We deduce that in Guinea, rainfall has a unimodal regime with peaks in August in each region. The thunderstorms variability is also bimodal with two peaks, one at the beginning of season and second at the end of season, respectively corresponding to Inter-Tropical Convergence Zone (ITCZ) arrival and return. It is noted that, this migratory movement of ITCZ is followed often by meteorological phenomena such as thunderstorms, etc.

EOFs and PCs rotated of rainfall and thunderstorms in Guinea

EOFs and PCs rotated of rainfall in Guinea

Figure 7 represents the EOFs (in the first column) and PCs (in the second column) of rainfall in Guinea for the period 1981-2010. The first mode EOFs1 (Figure 7a) corresponding to the PC1 (Figure 7b), highlights distribution pattern more or less uniform over the entire domain, with positive rainfall anomalies in Guinea where the variance is 25.1%. This means that the EOF1 pattern

shows us the overall strongest amplitudes of rainfall data. It corresponds to years characterized by positive rainfall anomalies (wet years). The PC1, indicates dry conditions at the beginning of climatological period (1981-1993) and wet conditions for 1994-2010 period, with the very wet year of 1994 which is consistent with the Figure 1. This means that the observed rainfall exhibited by EOFs1 pattern is related in majority to wet period.

The second mode pattern (Figure 7c) corresponding to PC2 (Figure 7d), reproduces a strong gradient of positive rainfall anomaly over the entire domain and highlights coastal of Guinea (LG), the south-eastern part (FG) with 22.3% of variance. These two regions represent the Guinean regions (map) where maximum rainfall amount is record. Around the Fouta Djallo Mountains, the negative rainfall anomalies are observed in the center explaining a deficit rainfall in this area. The wet patterns located in coastal part (LG) are explained by orographic behaviors and the oceanic influence, and the wet patterns around south-eastern (FG) are related to the forest impact. The corresponding PC2 shows very interannual rainfall variability compared to the PC1 with much fluctuation. The EOF3 (Figure 7e) represents 14.7% of variance with a different distribution compared to two previous modes. It shows an inter-regional dipole of rainfall, one at the coast (LG) and the other in forest area (FG).

However, the PC3 (Figure 7f) reveals some similarity in the interannual variability with PC2 with many fluctuations. The EOF4 (Figure 7g) clearly shows a distribution slightly similar to the second mode (EOF 2) with 12.9% of variance. And then, its corresponding PC4 (Figure 7h) indicates an inter-annual variability similar to PCs3. This means the adjacent EOFs are not well separated hence the North's rule of thumb is used to check them.

For this purpose, we checked the significance of each rainfall EOFs mode using North's rule of thumb for estimation of the eigenvalues (Figure 8). This rule informs that if a group of true eigenvalues (λ) lies within one or two $\Delta\lambda$ of each other, these eigenvalues form an "effectively degenerate multiplet", and sample eigenvectors (Dommenger et al., 2002). We notice on Figure 7 that no mode is concerned by this sampling where the difference ($\lambda - \Delta\lambda$, in green) is not one or two. We can conclude that the adjacent EOFs are physically separated from each other and they are not degenerate multiplet.

EOFs and PCs rotated of thunderstorms in Guinea

Figure 9 represent EOFs and PCs of thunderstorms in Guinea for the first four modes. The EOFs patterns for the first mode (Figure 9a) indicate an overall uniform positive anomaly of thunderstorms over the whole country with 38.5% of variance. EOF1 pattern shows a

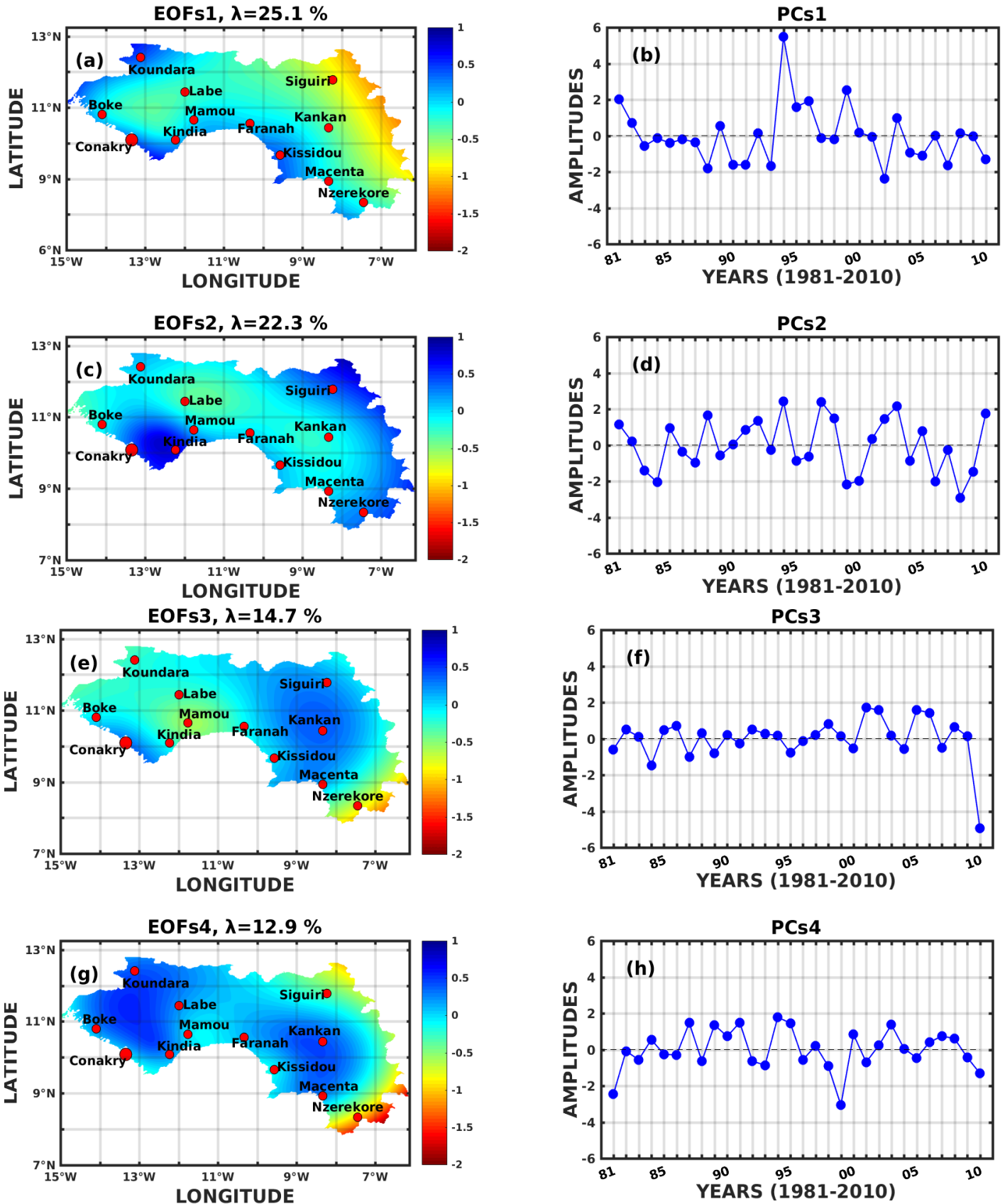


Figure 7. First four modes of the Rotated EOFs (REOFs) and the Rotated PCs (REOFs) of rainfall in Guinea. (a) EOF1 and (b) PC1, (c) EOF2 and (d) PC2, (e) EOF3 and (f) PC3, (g) EOF4 and (h) PC4. The X and Y axis of PCs are respectively anomalies and years.

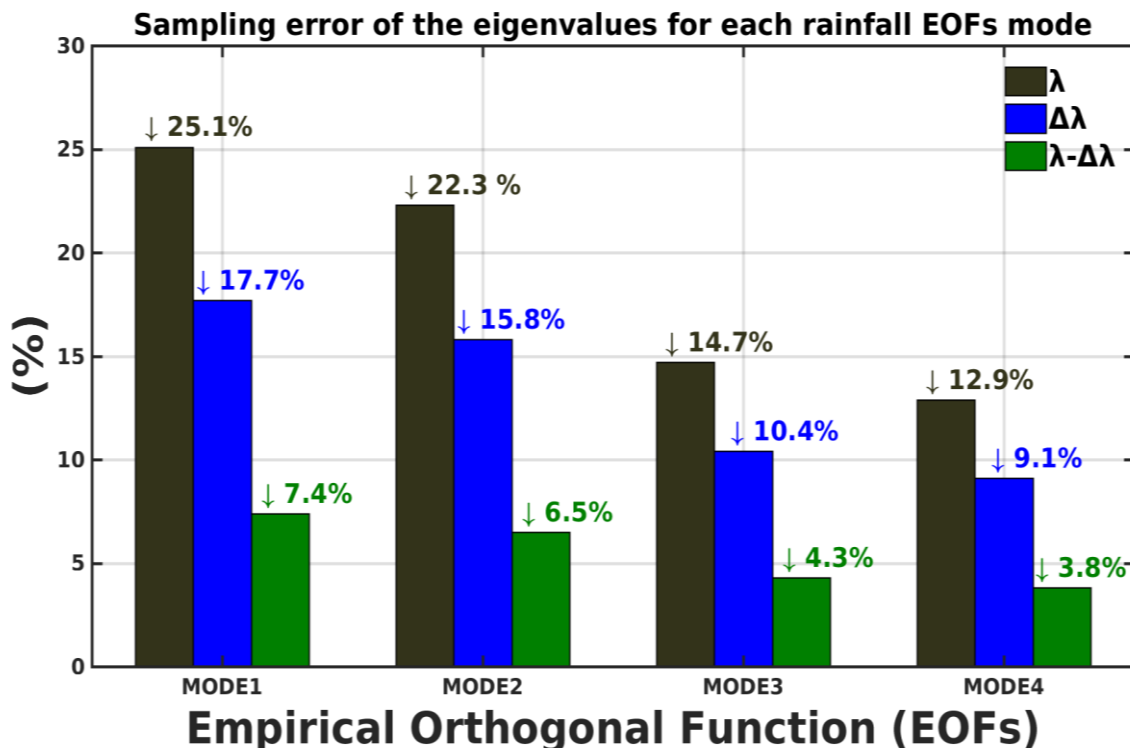


Figure 8. Sampling error of the eigenvalues for each rainfall EOF mode. Eigenvalues (λ , black), sampling error ($\Delta\lambda$, blue), difference between eigenvalues and sampling error ($\lambda - \Delta\lambda$, green). The X and Y axis are respectively EOFs and Percentage.

strong gradient everywhere over the coast (LG), Fouta Djallon (MG) and south (FG) which are areas where high occurrences of thunderstorms are recorded. This explains that EOF1 pattern shows the overall strongest amplitudes of thunderstorm data. Regarding corresponding PC1 (Figure 9b), a variability with a downward multi-year variability of thunderstorms is indicated during the 1988-2006 period which is close to what the Figure 4b has shown. It is for this reason that the observed thunderstorms in the country relative to the 1981-1993 period during which heavy thunderstorms are found.

The EOF2 pattern (Figure 9c) with 18.1% variance shows a dipole of negative anomalies of thunderstorm in Guinea: one in the western part (around the coast) in LG region and another in southern area (FG). Otherwise, the western part (LG), central part (Labe) and the northern area (MG) of Guinea have a common positive thunderstorm pattern with a zonal gradient. These areas are localities where the thunderstorms are recorded mainly during the beginning and the end of the season. Moreover, the corresponding PC2 (Figure 9d) illustrates a variability of thunderstorms like the PCs1 revealing a downward trend.

The EOF3 pattern (Figure 9e) with 14.5% of variance explained, has a structure different from the two previous modes with an opposite dipole compared to the second mode where the strong signal is found in the coastal part

of the country. However, the PC3 (Figure 9f) shows a similar variability to PC2, except for the period 2006-2010 with a downward multi-year variability like PC1. This configuration could be probably implied by climatic behavior, but we perform the North's rule of thumb below clarify this likeness modes. Finally, the EOFs corresponding to the fourth mode (Figure 9g) with 12.5% of variance, also presents a thunderstorm strong gradient of positive anomalies in the coastal part of Guinea and also in the central area (Mamou). The corresponding PC4 (Figure 9h) reveals a variability whose multi-year variability is mainly decreasing from 1989 up to 2001. Indeed, the strong negative signals of thunderstorm anomalies in East of the country concerns the 1989-2010 marked by a decline of thunderstorm events.

By testing the significance of each thunderstorm EOF mode using the North's rule of thumb for estimation of the eigenvalues. Each EOF will have different sampling requirements depending upon the nearness of neighboring eigenvalues (Dommenger et al., 2002). This rule indicates here that in groups or modes 3 and 4 of true eigenvalues (λ) that the difference ($\lambda - \Delta\lambda$) is inferior to two of each other, to form an "effectively degenerate multiplet", and sample eigenvectors (Figure 10). This confirms that there is no similarity in physics between EOFs 3 and 4. This means that adjacent EOFs of modes 3 and 4 are well separated and they are not degenerate

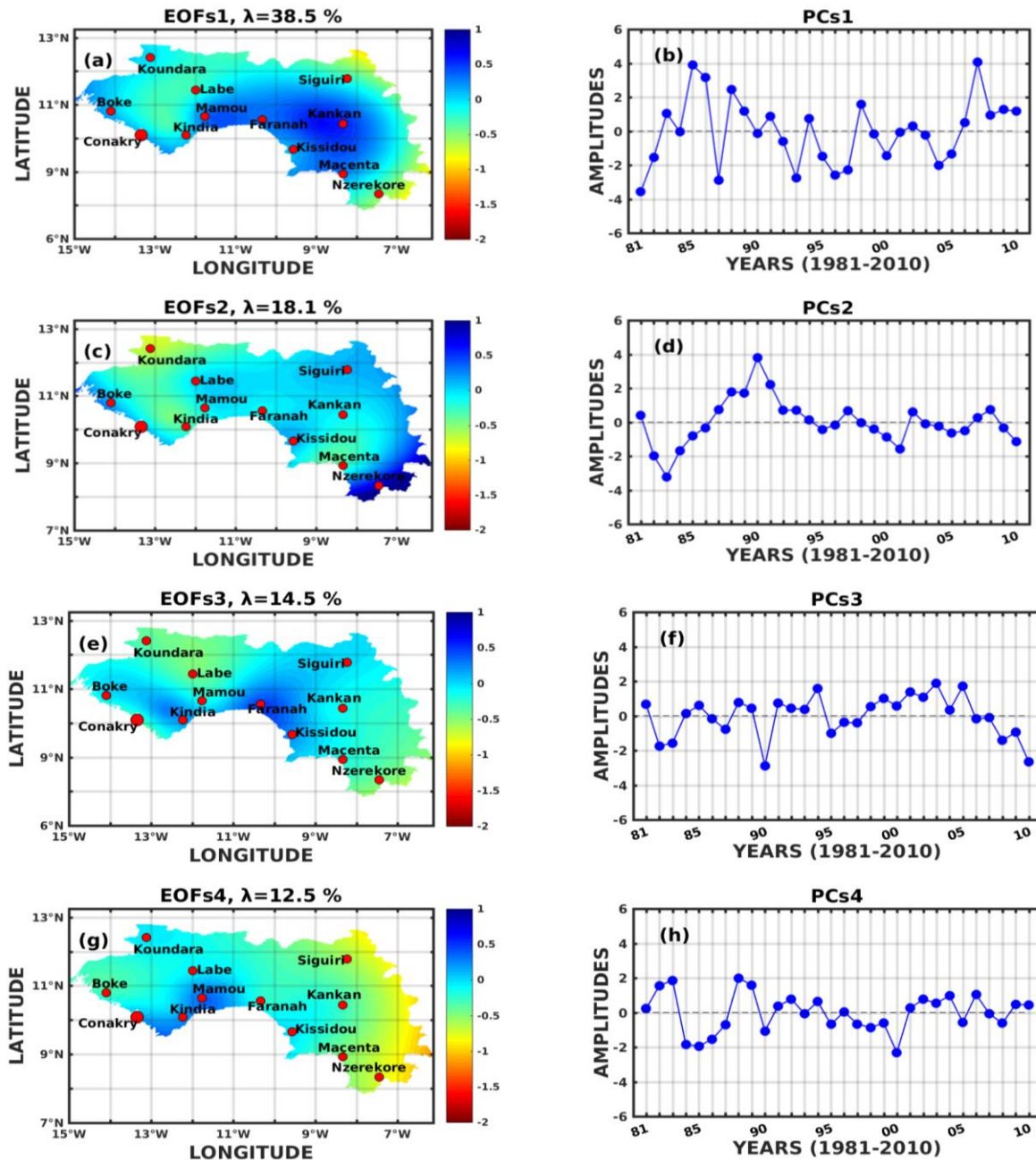


Figure 9. First four modes of the Rotated EOFs (REOFs) and Rotated PCs (RPCs) of thunderstorm in Guinea. (a) EOF1 and (b) PC1 (c) EOF2 and (d) PC2, (e) EOF3 and (f) PC3, (g) EOF4 and (h) PC4. The X and Y axis of PCs are respectively anomalies and years.

multiplet.

Relationship between rainfall and thunderstorms in Guinea

Firstly, we consider the overall rainfall and thunderstorms in Guinea; secondly, we divide the rainfall in two ranges:

weak rainfall ranging between 0 and 300 mm and heavy rain amount between 300 and 600 mm, and then correlate these respective rainfall time series with corresponding thunderstorms.

It was noticed that LG (Figure 11a) and MG (Figure 11b) regions are illustrated with a very good correlation coefficient between rainfall and thunderstorms (respectively $r=0.59$ and $r=0.78$) for a significance of than

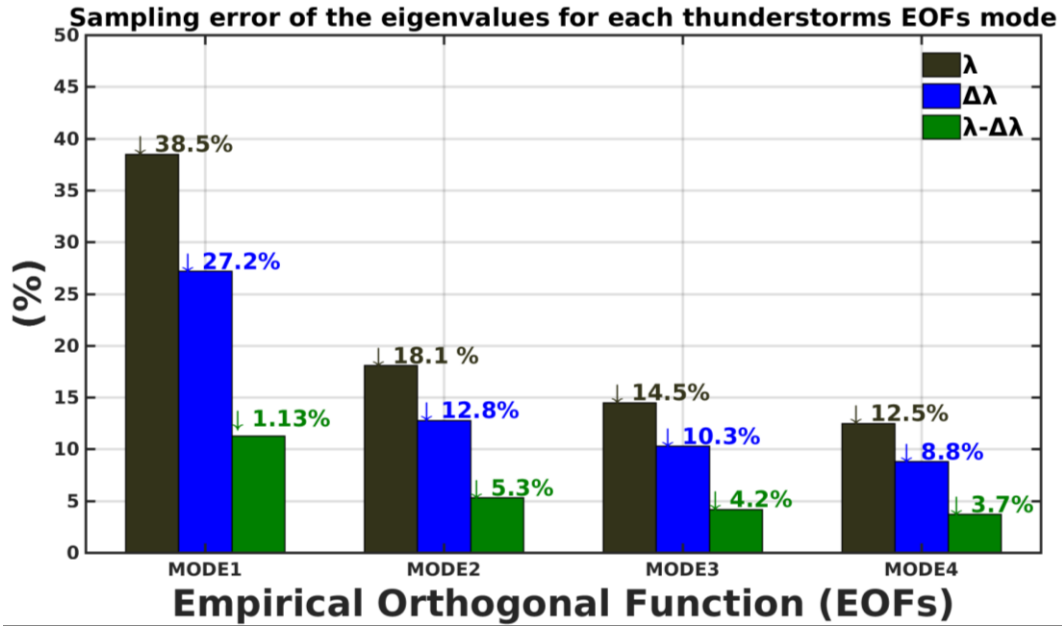


Figure 10. Sampling error of the eigenvalues for each thunderstorm EOF mode. Eigenvalues (λ , black), sampling error ($\Delta\lambda$, blue), difference between eigenvalues and sampling error ($\lambda - \Delta\lambda$, green). The X and Y axis are respectively EOFs and Percentage.

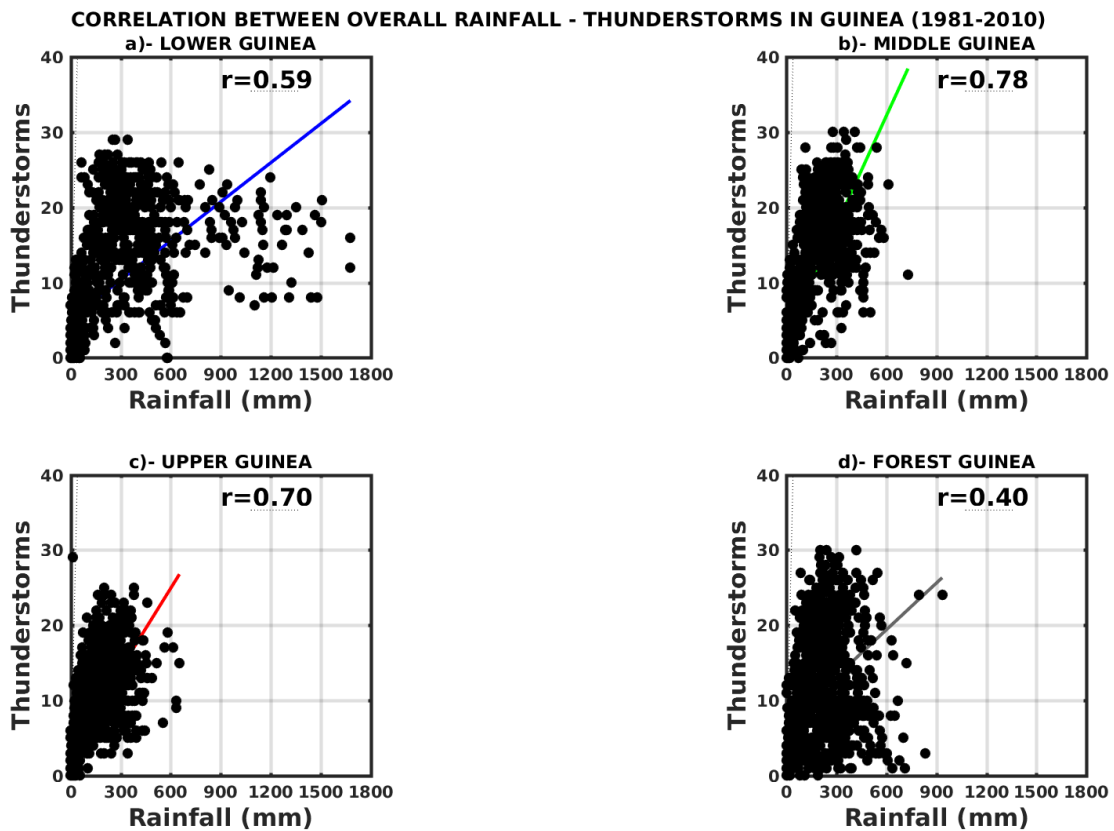


Figure 11. Correlation between rainfall and thunderstorms in Guinean regions: (a) Low Guinea (LG), (b) Middle Guinea (MG), (c) Upper Guinea (UG), (d) Forest Guinea (FG). The X and Y axis are respectively monthly rainfall amounts and monthly thunderstorms.

Table 2. Significant correlation between rainfall and thunderstorms by region with their respective stations.

Area and station	Parameter	Correlation (r)	Significance (%)	
Low Guinea	Low Guinea	Rainfall-Thunderstorm	0.59	>95
	Boke	Rainfall-Thunderstorm	0.68	>95
	Conakry	Rainfall-Thunderstorm	0.58	>95
	Kindia	Rainfall-Thunderstorm	0.75	>95
Middle Guinea	Middle Guinea	Rainfall-Thunderstorm	0.78	>95
	Koundara	Rainfall-Thunderstorm	0.80	>95
	Labe	Rainfall-Thunderstorm	0.84	>95
	Mamou	Rainfall-Thunderstorm	0.72	>95
Upper Guinea	Upper Guinea	Rainfall-Thunderstorm	0.70	>95
	Faranah	Rainfall-Thunderstorm	0.77	>95
	Kankan	Rainfall-Thunderstorm	0.69	>95
	Siguiri	Rainfall-Thunderstorm	0.59	>95
Forest Guinea	Forest Guinea	Rainfall-Thunderstorm	0.40	>95
	Kissidou	Rainfall-Thunderstorm	0.63	>95
	Macenta	Rainfall-Thunderstorm	0.33	>95
	Nzérékoré	Rainfall-Thunderstorm	0.37	>95

95%. However, rainfall and thunderstorms relationship is more important in MG region than in LG region. It means that 35% ($r^2=0.35$) and 61% ($r^2=0.61$) of rainfall in LG and in MG, respectively, are stormy originated. This 61% correlated rainfall with thunderstorms in MG, is visible on Figure 6b where even in full monsoon (August) stormy activities persist in this region. These stormy activities are decreasing in the other three geophysical regions, which could be due to the influence of Fouta Djallon massifs (orography). It was also observed in UG (Figure 11c) and FG (Figure 11d) regions, that there are significant correlation of 0.70 and 0.40, respectively. It is therefore deduced that 40% ($r^2=0.40$) and 16% ($r^2=0.16$) of rainfall amounts storm derived from these respective regions and proportions. These results imply that the relationship of rainfall and thunderstorm in MG is stronger as compared to LG, UG and FG regions Table 2.

Relation between weak rainfall (0-300 mm) and thunderstorms in Guinea

Here, we correlate weak rainfall between 0-300 mm (Figure 12) and corresponding thunderstorm occurrences. In the four geophysical regions of Guinea (LG, MG, UG and FG), we note that rainfall is well correlated with thunderstorms. LG (Figure 12a) and MG (Figure 12b) regions show a significance correlation respective of $r=0.85$ and $r=0.86$. It means that 72% ($r^2=72$) of these weak rainfall in LG and 74% ($r^2=74$) in MG are stormy rainfall.

UG (Figure 12c) and FG (Figure 12d) regions indicate a

good correlation of $r=0.76$ and $r=0.65$, respectively. This informs that in UG and FG regions 58% ($r^2=0.58$) and 42% ($r^2=0.42$) of weak rainfall are thunderstorms originated. We note that in Guinean geophysical regions, the weak rainfall is from stormy convective systems.

Relation between heavy rainfall (300-600 mm) thunderstorms in Guinea

For the heavy rainfall amounts between 300 and 600 mm (Figure 13), which we correlated with thunderstorms in each Guinea region, LG region (Figure 13a) and MG region (Figure 13b) show low to very low correlations and negative, respectively $r=-0.23$ and $r=-0.04$. This means that in LG and MG regions, the heavy precipitation is not stormy originated and evolve in an opposite way. Concerning UG (Figure 13c) and FG (Figure 13d) regions, we note also negative and very low correlations between heavy rainfall and thunderstorms, respectively $r=-0.03$ and $r=-0.19$. We find that these correlations are all negative and relatively weak, which means that when rainfall are high, the links between thunderstorms and rain are no longer linear. That is to say, these two phenomena show an opposition in their evolution one grows the other decreases and conversely.

Conclusion

In general, during the climatological period (1981-2010),

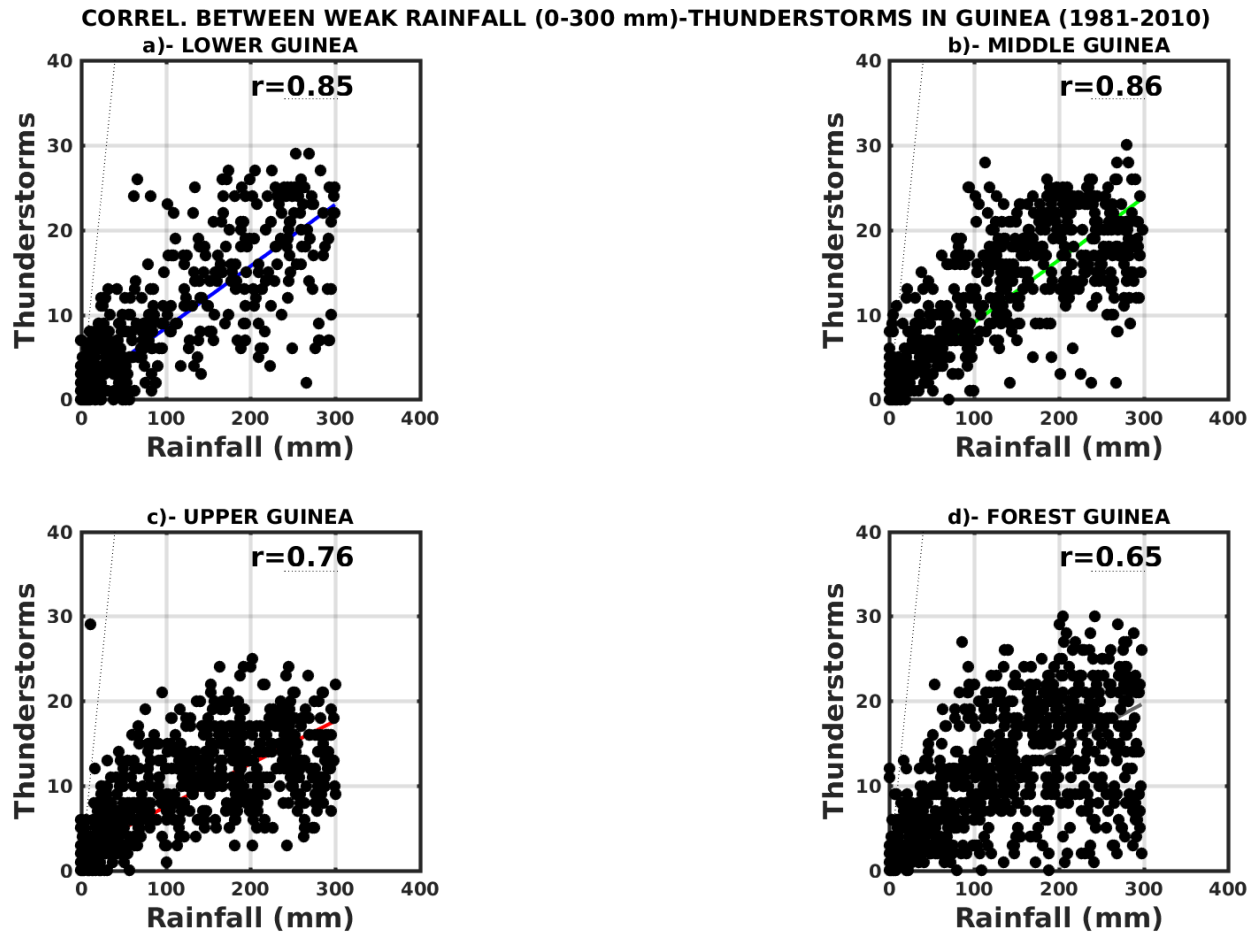


Figure 12. Correlations between the weak (0-300mm) rainfall and thunderstorms in Guinean regions: (a) Low Guinea (LG), (b) Middle Guinea (MG), (c) Upper Guinea (UG), (d) Forest Guinea (FG). The X and Y axis are respectively monthly rainfall amounts and thunderstorms.

the SPI highlights that Guinea also experienced the 1970's drought like the Sahel, a period followed by a wet rainfall regime including the very rainy year of 1994. Moreover, the STI exhibits a decrease of thunderstorms in Guinea during the rainfall recovery period with heavy rainfall but low correlated with thunderstorms. Regarding the four geophysical regions of Guinea, we have shown that the three ones (LG, MG, UG) experienced these episodes of drought like Sahel. The decline trend significantly for the thunderstorms in FG is compared to other regions of country. The recovery rainfall period is shown in all the different geophysical regions of Guinea, but particularly in MG where the findings are very coherent with results revealed in the overall Guinea. Otherwise, it is noted with the STI that all regions are concerned by the decline of thunderstorms during the rainfall recovery period, mainly in the FG region where results are better in agreement with the global STI. This decline would be due to heavy rainfall which is less correlated with thunderstorms.

In Guinea, the seasonal mean rainfall cycle likely indicates similar regimes in the four geophysical regions with an absolute peak in August. We conclude that in Guinea, rainfall has a unimodal regime with a peak in August. Regarding the thunderstorms, the seasonal mean cycle exhibits a bimodal evolution with two peaks, one at the beginning of season and second at end of season, respectively corresponding to arrival and ITCZ return.

In the EOFs and PCs analyses, mode 1 exhibits a homogeneous overall pattern of rainfall over Guinea and the expansion coefficient (PC1) confirms the drought and the rainfall recovery. This result is also shown with the SPI. Modes 3 and 4 of EOFs indicate a rainfall dipole in the wetter two regions (LG and FG) of Guinea. These two regions represent the Guinean regions where record maximum rainfall is observed. The first one is under oceanic and orography influenced implies the wet patterns in the coastal part (LG) and a second wet pattern around south-eastern (FG) is related to forest impact.

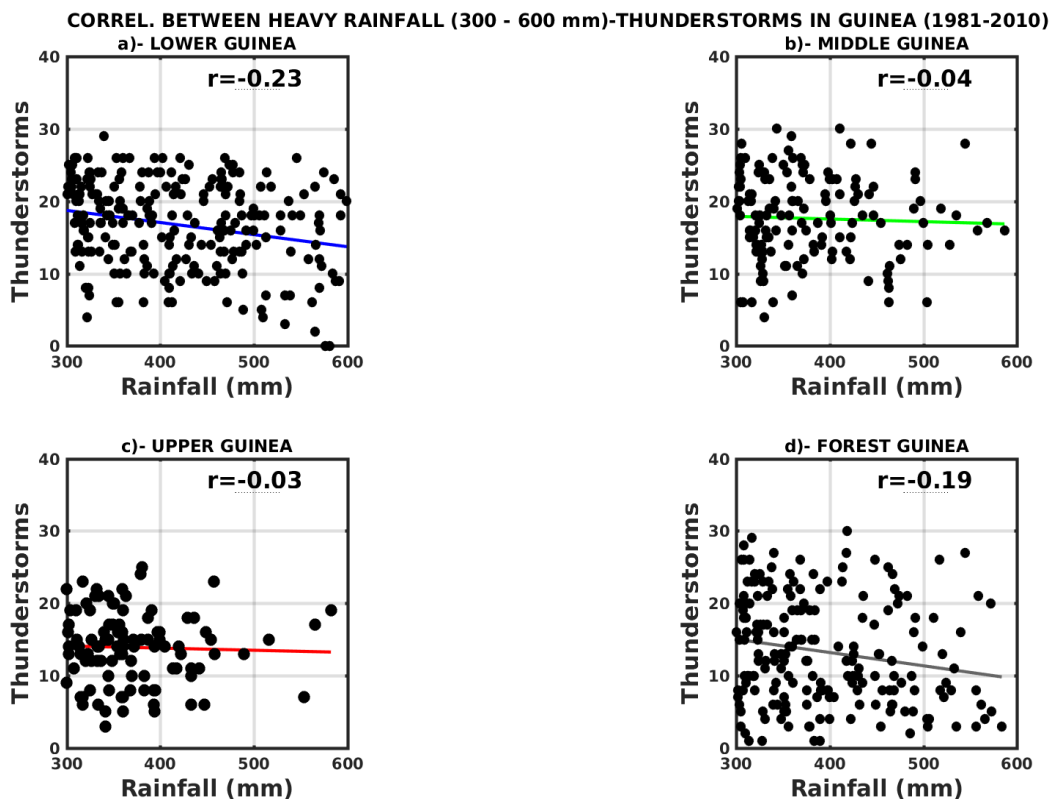


Figure 13. Correlations between heavy rainfall (300-600 mm) and thunderstorms in Guinean's regions : (a) Low Guinea (LG), (b) Middle Guinea (MG), (c) Upper Guinea (UG), (d) Forest Guinea (FG). The X and Y axis are respectively monthly rainfall amounts and thunderstorms.

Regarding the thunderstorms, mode 1 indicates a homogeneous pattern over Guinea with a strong gradient everywhere over the coast (LG), Fouta Djallon (MG) and south (FG) which are areas where high occurrences of thunderstorms are recorded. The corresponding PC1 confirms more or less a downward, and we note the same things on PCs2 to 4 found with the thunderstorm index too. This means that effectively the multi-year variability is decreasing, confirming that the second mode is better than others. According to the North's rule of thumb, we showed that concurrent rainfall and thunderstorm EOFs are well separated from each other with neither difference of one or two between eigenvalue and sampling error. These differences are either greater or less than 1.

Considering correlations between rainfall and thunderstorms in Guinea, significant coefficients are highlighted in LG, UG and MG, whereas in FG region the correlation values are low. In fact, rainfall in these areas increase with thunderstorms, that means that stormy convective systems mainly take place in these regions. Although the percentage of stormy rainfall in FG is lower. However, the weak rainfall and thunderstorms showed strong correlation values in the 4 regions varying between 0.65 and 0.86. This means that in Guinea, the

weak rainfall are of stormy origin. Indeed, heavy rainfall and thunderstorms are less correlated with the low values of correlation and negative. This shows an evolution opposition of the two phenomena, that is to say when one grows while the other decreases and vice versa. Meaning heavy rainfall is not necessarily related to thunderstorms sometimes, but with other types of convective systems like vortex or large mesoscale systems (Jenkins et al., 2008). The significant correlations between rainfall and thunderstorms in the FG should be linked to the forest and orographic patterns which are potential storm triggers. This is consistent with Sall et al. (1999) and Mathon and Laurent (2001) results which showed that in Africa, the main mountainous areas generally correspond to the maximum of cloud cover.

CONFLICT OF INTERESTS

The authors have declared any conflict of interests.

ACKNOWLEDGEMENTS

This study was funded by SCAC (Service de Cooperation

et d'Action Culturelle de l'Ambassade de France en Guinée), AFIMEQG (Afrique pour l'Innovation, Mobilité, Echange, Globalisation et Qualité) of European Union (EU) which are institutions of mobility program and cooperation in the field of Higher Education and ESP/LPAOSF (École Supérieure Polytechnique/Laboratoire de Physique de l'Atmosphère et de l'Océan Siméon Fongang) in Senegal. The authors present their warm thanks to these institutions, whose scholarship awarded to Ibrahima Kalil Kante permits the achievement of this paper. In addition, the authors would like also to thank the NMS (Nationale Meteorology Service) of Guinea and University Gamal Abdel Nasser of Conakry, but also the LPAOSF (Laboratoire de physique de l'Atmosphère et de l'Océan Siméon Fongang) in Senegal who welcomed Ibrahima Kalil Kante in the framework of his Ph.D studies.

REFERENCES

- Abdi H, Williams LJ (2010). Principal component analysis. *Wiley Interdisciplinary Reviews: Computational Statistics* 2(4):433-459.
- Ali A, Lebel T (2009). The Sahelian standardized rainfall index revisited. *International Journal of Climatology* 29(12):1705-1714.
- Ali A, Thierry L, Abou A (2008). Signification et usage de l'indice pluviométrique au Sahel. *Science et Changements Planétaires/Sécheresse* 19(4):227-235.
- Béavogui K, Badiane D, Sall SM, Diaby I (2011). Approche climatologique des phénomènes pluvio-orageux en Guinée. *Journal des Sciences Pour l'Ingénieur* N°13:71-77.
- Bouroche JM, Saporta G (1987). *Analyse des données*, Vol. 1854. Presses Universitaires de France, Collection climatique au Gabon en 1984. *La Météorologie* 8:36-45.
- Cattell RB (1966). The scree test for the number of factors. *Multivariate Behavioral Research* 1(2):245-276.
- Christian H, Blakeslee R, Goodman S, Mach D, Stewart M, Buechler D, Boccippio DJ (1999). The lightning imaging sensor. In NASA Conference Publication NASA. pp. 746-749.
- Dawson A (2016). eofs: A library for eof analysis of meteorological, oceanographic, and climate data. *Journal of Open Research Software* 4:1.
- Deser C, Blackmon ML (1995). On the Relationship Between Tropical and North Pacific Sea Surface Temperature Variations. *Journal of Climate* 8(6):1677-2680.
- Dommenget D, Latif M (2002). A cautionary note on the interpretation of EOFs. *Journal of Climate* 15(2):216-225.
- Frenken K (Ed.). (2005). *Irrigation in Africa in figures: AQUASTAT Survey*, Food and Agriculture Organisation. Vol. 29.
- Giannini A, Saravanan R, Chang P (2003). Oceanic forcing of Sahel rainfall on interannual to interdecadal time scales. *Science* 302(5647):1027-1030.
- Grist JP, Nicholson SE (2001). A study of the dynamic factors influencing the rainfall variability in the West African Sahel. *Journal of Climate* 14(7):1337-1359.
- Hulme M (1992). Rainfall changes in Africa: 1931–1960 to 1961–1990. *International Journal of Climatology* 12(7):685-699.
- Janicot S, Fontaine B (1993). L'évolution des idées sur la variabilité inter annuelle récente du cycle de l'eau atmosphérique en Afrique de l'Ouest. *La météorologie*.
- Jenkins GS, Pratt AS, Heymsfield A. (2008). Possible linkages between Saharan dust and tropical cyclone rain band invigoration in the eastern Atlantic during NAMMA-06. *Geophysical Research Letters* 35:8.
- Kaiser HF (1958). The varimax criterion for analytic rotation in factor analysis. *Psychometrika* 23(3):187-200.
- Keyantash J, Dracup JA (2002). The quantification of drought: an evaluation of drought indices. *Bulletin of the American Meteorological Society* 83(8):1167-1180.
- Lamb PJ, Pepler RA (1992). Further case studies of tropical Atlantic surface atmospheric and oceanic patterns associated with sub-Saharan drought. *Journal of Climate* 5(5):476-488.
- Laing AG, Fritsch JM, Negri AJ (1999). Contribution of mesoscale convective complexes to rainfall in Sahelian Africa: Estimates from geostationary infrared and passive microwave data. *Journal of Applied Meteorology* 38(7):957-964.
- Laurent H, d'Amato N, Lebel T (1998). How important is the contribution of the mesoscale convective complexes to the Sahelian rainfall? *Physics and Chemistry of the Earth* 23(5-6):629-633.
- Le Barbé L, Lebel T, Tapsoba D (2002). Rainfall variability in West Africa during the years 1950–1990. *Journal of Climate* 15(2):187-202.
- Loua RT, Beavogui M, Benchérif H, Bamba Z, Amory-Mazaudier C (2017). *Climatology of Guinea: Study of Climate Variability in N'zerekore*. *Journal of Agricultural Science and Technology (JAST)* 7:4.
- Louvet S, Paturol JE, Mahé G, Vigaud N, Roucou P (2011). Variabilité spatio-temporelle passée et future de la pluie sur le bassin du Bani en Afrique de l'Ouest. *Hydro-Climatology: Variability and Change*, pp. 125-130.
- Mathon V, Laurent H (2001). Life cycle of the Sahelian mesoscale convective cloud systems. *Quarterly Journal of the Royal Meteorological Society* 127:377-406.
- Mestas-Nuñez AM (2000). Orthogonality properties of rotated empirical modes. *International Journal of Climatology: A Journal of the Royal Meteorological Society* 20(12):1509-1516.
- McKee TB, Doesken NJ, Kleist J (1993). The relationship of drought frequency and duration to time scales. In *Proceedings of the 8th Conference on Applied Climatology*, Boston, MA: American Meteorological Society 17(22):179-183.
- Mohino E, Rodriguez-Fonseca B, Mechoso C, Gervois S, Ruti P, Chauvin F (2010). West Africa Monsoon response to Tropical Pacific sea surface anomalies. *Journal of Climate*.
- Nicholson SE (2013). The West African Sahel: A review of recent studies on the rainfall regime and its interannual variability. *ISRN Meteorology*.
- Nicholson S (2005). On the question of the "recovery" of the rains in the West African Sahel. *Journal of Arid Environments* 63(3):615-641.
- Nicholson S (2000). Land surface processes and Sahel climate. *Reviews of Geophysics* 38(1):117-139.
- North GR, Thomas LB, Robert F (1982). Cahalan, and Fanthune J. Moeng., Sampling errors in the estimation of empirical orthogonal functions. *Monthly Weather Review* 110(7):699-706.
- Petersen WA, Rutledge SA (1998). On the relationship between cloud-to-ground lightning and convective rainfall. *Journal of Geophysical Research: Atmospheres* 103(D12):14025-14040.
- Poccard-Leclercq I (2000). *Etude diagnostique de nouvelles données climatiques: les réanalyses. Exemples d'application aux précipitations en Afrique Tropicale*. (Doctoral dissertation, Université de Bourgogne) 255:30-31.
- Rakov VA, Uman MA (2003). *Lightning: physics and effects*. Cambridge University Press.
- Richman MB (1986). Rotation of principal components. *Journal of Climatology* 6(3):293-335.
- Richman M (1981). Oblique rotated principal components: an improved meteorological map typing technique? *Journal for Climate and Applied Meteorology* 20(1):1145-1159.
- Sall SM, Gaye AT, Fongang S, Viltard A (1999). Génération et dissipation des systèmes convectifs sur l'Afrique de l'Ouest durant l'été 1993. *Ass. Int. Clim.* 12:422-429.
- Sheridan SC, Griffiths JF, Orville RE (1997). Warm season cloud-to-ground lightning precipitation relationships in the south-central United States. *Weather and Forecasting* 12(3):449-458.
- Solomon S, Qin D, Manning M, Averyt K, Marquis M (Eds.). (2007). *Climate change 2007-the physical science basis: Working group I contribution to the fourth assessment report of the IPCC* Cambridge university press. P. 4.
- Soula S, Sauvageot H, Molinie G, Mesnard F, Chauzy S (1998). The CG lightning of a storm causing a flash-flood. *Geophysical Research Letters* 25(8):1181-1184.

- Zhou T, Yu R, Li H, Wang B (2008). Ocean forcing to changes in global monsoon precipitation over the recent half-century. *Journal of Climate* 21(15):3833-3852.
- Zhou Y, Qie X, Soula S (2002). A study of the relationship between cloud-to-ground lightning and precipitation in the convective weather system in China. In *Annales Geophysical* 20(1):107-113.